

EFFECT OF SUBSTRATE TEMPERATURE ON THE GALVANOMAGNETIC, PHOTOELECTRICAL AND OPTICAL PROPERTIES OF $\text{Pb}_{0.8}\text{Sn}_{0.2}\text{Te}$ THIN FILMS

M. ABDEL RAFEA^{*}, F.S.TERRA^a, M. MOUNIR^b, R. LABUSCH^c

Electronic Materials Dep., Advanced Technologies and New Materials Institute, Mubarak City for Scientific Research and technology Applications, P.O. 21934 New Borg El-Arab, Alexandria,

^aSolid State Physics Dep., National Research Centre, Dokki, Cairo, Egypt

^bPhysics Department, Faculty of Science, Cairo University.

^cInstitute fuer physic und physikalische Technologien, TU-Clausthal, Germany.

The effect of substrate temperature on the electrical, photoconductivity, galvanomagnetic and optical properties of $\text{Pb}_{0.8}\text{Sn}_{0.2}\text{Te}$ films was studied. The electrical resistivity decreases one order of magnitude as T_s increases and nearly unchanged with the temperature from 77-300 K. The carrier's concentration decreases by 2-3 orders of magnitude as T_s increases. It was observed that the carriers are p-type due to a slight excess Te in the films and nearly unchanged with temperature. The Hall mobility was observed to increase by 1-2 orders of magnitudes as T_s increases. The average optical transmittance was found to be 30 % for films deposited at room temperature and increases close to 90-100 % as T_s increases to 673 K. The optical band gap was calculated and was found to be quite higher than those for single crystal which decreases as T_s increases to be close to the band gap of the single crystal as films annealed at 673 K. The IR photoconductivity measurements shows that high photosensitivity at low temperature was observed while it was smaller at room temperature. The determined band gap from the photoconductivity measurements is similar to the obtained from the optical method while both of them are higher than the calculated from the semi-empirical formula of $\text{Pb}_{0.8}\text{Sn}_{0.2}\text{Te}$ crystals. This difference was decreased as the substrate temperature increased and mainly depends upon the carrier's concentration. This was explained by the Burstein-Moss effect of low effective mass and/or high carriers concentration semiconductors.

(Received March 17, 2008; accepted April 3, 2009)

Keywords: Lead Tin Telluride, Thin Films, Structure, Electrical, Optical Properties, Photoconductivity, Energy Gap and Substrate Temperature.

1. Introduction

Semiconducting PbSnTe material is important due to its wide applications in infrared technologies, night vision, IR detectors, photodiodes or photoconductors. The difficulty in preparing $\text{Pb}_{0.8}\text{Sn}_{0.2}\text{Te}$ thin films is the controlling of Te due to its low vapor pressure. Normally Te rich films are obtained which produces p-type semiconductors with high carrier's concentration. A lower carrier concentration film is benefit in most of the applications. Dawar *et al* [1] reported that $\text{Pb}_{1-x}\text{Sn}_x\text{Te}$ with $x=0.18-0.25$ thin films are interesting for IR detectors and laser diodes. $\text{Pb}_{1-x}\text{Sn}_x\text{Te}$ is a direct-allowed narrow gap semiconductor, its band gap changes with temperature, T and composition, x according to the semi-empirical formula [2]:

^{*}Corresponding author: m.abdelrafea@mucsat.sci.eg

$$E_g(x, T) = 0.19 - 0.543x + \frac{T^2 4.5 \times 10^{-4}}{(T + 50)} \quad (1)$$

$\text{Pb}_{1-x}\text{Sn}_x\text{Te}$ is a cubic structure. The lattice dimensions $a(\text{\AA})$ at $x=0.0$ and $x=1.0$ are 6.454 and 6.313 \AA respectively. The lattice dimension of the $\text{Pb}_{1-x}\text{Sn}_x\text{Te}$ follows the Vegard's law.

$$a(x) = (1-x) \times 6.454 + x \times 6.313 \text{ \AA} \quad (2)$$

This means that at $x=0.20$ the unit cell dimension is 6.426 \AA . Tao *et al* [3] have reported that photoconductivity of these films can be observed after annealing in Pb/Sn rich vapor to reduce the carrier concentration to $\sim 10^{17} \text{ cm}^{-3}$.

The electrical and galvanmagnetic properties of $\text{Pb}_{1-x}\text{Sn}_x\text{Te}$ single crystals were studied by many researchers for IR sensor [4-7]. The effect of magnetic field upon the Hall coefficient of $\text{Pb}_{0.8}\text{Sn}_{0.2}\text{Te}$ Indium doped single crystals [8]. Ostroborodova *et al* [9] have studied the Galvanmagnetic properties of $\text{Pb}_{0.95}\text{Sn}_{0.05}\text{Te}$ crystals and the dependence of the carriers concentration upon the band gap was studied by Zemel *et al* [10], it was observed that at low carriers concentration, minimum E_g was obtained independent upon the carriers concentration, while E_g increases as the carriers concentration increases due to the partial filling of the valence band or the so called the Burstein-Moss shift [11,12]. In a previous work of PbSnTe pressed powder and flash evaporated films [13,14], as the composition increases from 0.0 to 0.4, the mobility increases three times while the carriers concentration increases three orders of magnitudes. Flash evaporation technique was observed to be the most control process for composition and content while layered structure was observed to lower the film quality. A similar mobility and carrier's concentration were obtained for thin films and the pressed samples, while a high photoconductivity was observed at lower temperature for the films. The aim of this work is to prepare $\text{Pb}_{0.8}\text{Sn}_{0.2}\text{Te}$ photoconductors which sensitive at the 3-5 μm spectrum range with film quality better than those prepared by flash evaporation and better controlled absorption edge wavelength by minimization of the band gap shift due to high carriers concentration [excess Te effect].

2-Experimental

$\text{Pb}_{0.8}\text{Sn}_{0.2}\text{Te}$ ingot material was prepared from melt in evacuated silica ampoules under He atmosphere evacuated at 10^{-6} . Pb, Sn and Te of 6N (Alfa Aesar Johnson Matthey GmbH Germany) were used as the raw materials. The composition was set to be 0.2 by weighting elements using 0.1 mg accuracy balance. The ampoule was placed in a calibrated furnace using thermocouple (Chromel-Alumel) at 1223 ± 5 K and shacked every 20 min for homogenization. This temperature was reached using a rate of 10 deg/min. after 2 h melting time, the ingot was solidified rapidly at 1073 K to prevent segregation then the temperature is decreased with the with slower rate by turning the furnace off and close the furnace to cool down slowly. A fine powder of $\text{Pb}_{0.8}\text{Sn}_{0.2}\text{Te}$ was made from the ingot materials by grinding in a mortar. The powder is used for XRD measurements and the remaining powder was pressed as tablets under a pressure of 10 Ton/cm² for SEM-EDX measurements and thin film deposition. Thin films were prepared from the ingot materials using the electron beam evaporation unit (Edwards-England) at different substrate temperatures, $T_s=300, 373, 473, 573$ and 673 K. The material was put in a thick molybdenum crucible. The source to substrates distance was adjusted to be 19 cm and the substrates were fixed at a circle on the substrate holder of 10 cm diameter in order to produce films with the same thickness and homogeneity. The films thickness and evaporation rate were measured during the evaporation process by thickness monitor which they are controlled by the electron gun current.

Glass substrates was cleaned by ultrasonic cleaner using fresh chromic acid, distilled water, detergent, distilled water then centrifuged to remove water from the substrate surface. KBr single crystal was obtained from "Korth" GmbH for IR measurements, the crystal was cleaved at (111) plane, and FT-IR spectrophotometer (Perkin Elmer FT-IR spectrometer 1725 x) was used.

The homogeneity of the films was tested by EDX measurement at 5 points on the film surface. The relative change in the composition or Te content does not exceed 4-6 %. The electrodes were made from In metal by thermal vacuum evaporation. Films of $x=0.20$ were prepared under the following conditions:- thickness $\sim 0.8 \mu\text{m}$, vacuum $\sim 2 \times 10^{-6}$ Torr and evaporation rate $\sim 25 \text{ \AA/s}$. The dimensions of the Hall Effect samples are 18 mm length, 2 mm width, while the dimensions of the photoconductivity samples are 10 mm width and 20 mm length. The photoconductivity measurements were carried out in the temperature range 77-300 K under monochromatic IR wavelengths in the range from 2.5-12 μm with calibrated output intensity by Pyro-electric detector. Hall mobility and carriers concentration was measured at magnetic field 8 KGauss and temperature range 100-300 K.

3. Results and discussion

3.1 Structure

the scanning electron micrograph shows that high quality films was obtained by the electron beam evaporation technique . There is no characteristic morphologies at the film surface such as cracks, peels, grains ...etc. in both high and low substrate temperatures. Elemental composition measurements using the EDX unit shows that the compositions of both ingot and films are nearly the same, while Te content in the films increases higher than the stoichiometric value as shown in Table (1).

Table 1. Variation of the composition and Te content with T_s

T_s K	300	373	473	573	673
Te	1.137	1.138	1.111	1.119	1.116
x	0.237	0.241	0.230	0.232	0.232

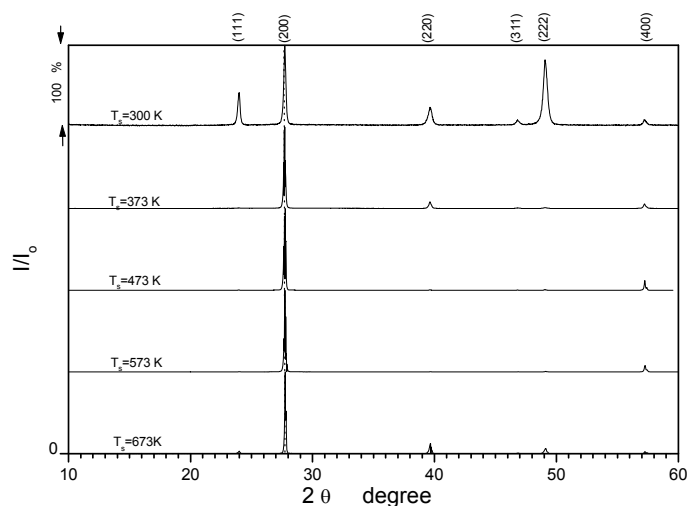


Fig. 1. XRD pattern for $\text{Pb}_{0.80}\text{Sn}_{0.20}\text{Te}$ films prepared at different T_s .

Polycrystalline cubic structure of PbSnTe crystalline system with unit cell dimension close to the calculated from Equation (2) was observed, and preferred orientation (200) was

characterized and shown in Fig.(1). Films deposited at room temperature possess preferred orientation (200) besides considerable intensities for the reflections at the peaks (220), (111), (311), (222) and (400). As substrate temperature increases up to 673 K, all peaks other than (002) vanishes and (200) sharper peak was observed. This confirms the re-crystallization and re-orientation process besides the crystallite size increasing. The average crystallite size, L , of the films is calculated from the Scherrer's equation which is given by:

$$L = \frac{0.94\lambda}{\sqrt{\Delta_{sample}^2 - \Delta_{Si}^2} \cdot \cos(\theta)} \quad (3)$$

Where Δ_{sample} and Δ_{Si} are the peak width at half maximum intensities for sample and silicon, respectively. Silicon single crystal, defect free, was used for determination the instrumental broadening, λ is the X-ray wavelength (CuK α 1). As shown in Fig.(2), It was found that the crystallite size is 50 nm at $T_s=300-473$ K and increases to 85 nm at higher substrate temperature.

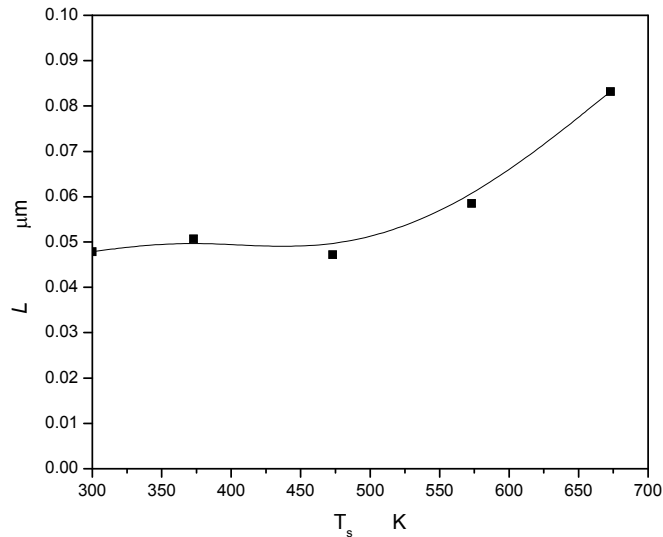


Fig. 2. Crystallite size dependence upon T_s for $Pb_{0.80}Sn_{0.20}Te$ films.

Table 2. The interplanar spacings d_{hkl} for films with $x=0.2$.

T_s (K)	Eg(100 K)	Eg(150 K)	Eg(200 K)	Eg(250 K)	Eg(300 K)
300	0.2219	0.2211	0.226	-----	-----
373	0.2175	0.2186	0.2249	0.2218	0.2201
473	0.1787	0.2069	0.2112	0.2170	0.2264
573	0.1308	0.1493	0.1527	0.160	0.218
673	0.1476	0.1471	0.1600	0.192	0.215
E(x,T)	0.111	0.1320	0.1534	0.175	0.197

3.2 Galvanomagnetic properties

The electrical resistivity changes slightly with cooling which indicates that the carriers concentration or mobility has weak dependence upon measuring temperature. The variation of the room temperature resistivity with substrate temperature is illustrated in Fig.(3) showing that resistivity increases from 10^{-2} - $10^{-1}\Omega\cdot\text{cm}$ when the substrate temperature increases from 300-673 K. The room temperature resistivity dependence upon the substrate temperature is quite similar as the behavior of crystallite size with substrate temperature. It is expected that a similar behavior of hall mobility takes place.

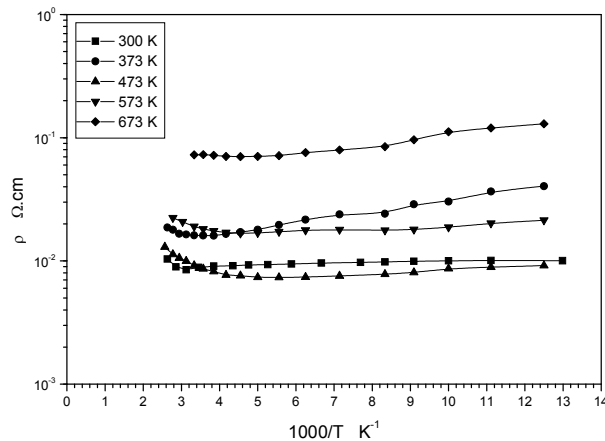


Fig. 3. Resistivity dependence upon temperature for $Pb_{0.80}Sn_{0.20}Te$ films deposited at different substrate temperatures.

The temperature dependence of the Hall mobility for films deposited at different substrate temperatures is shown in Fig.(4). The lowest Hall mobility is obtained for films deposited at $T_s=300$ K, which increases 1-2 order of magnitude when the substrate temperature increases up to 673 K. It is expected that crystallization (or growth) process occurs, leading to a decrease of the defects and consequently a decrease of the carriers scattering at the defects.

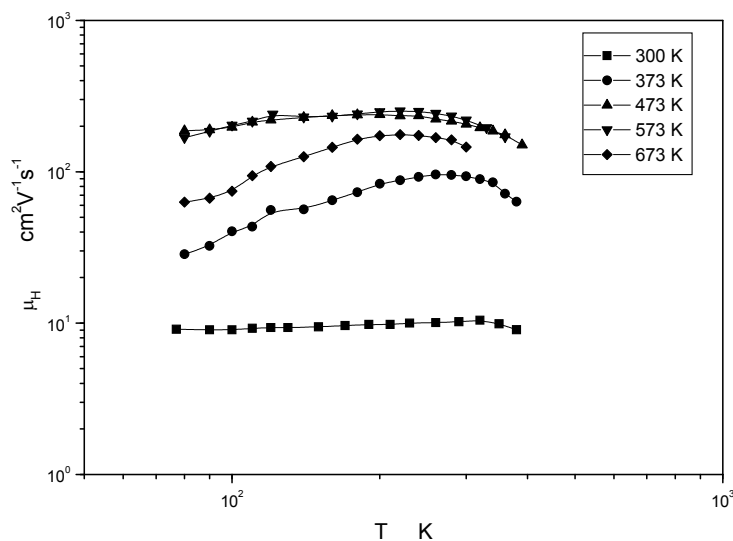


Fig. 4. Temperature dependence of the Hall mobility for $Pb_{0.80}Sn_{0.20}Te$ films.

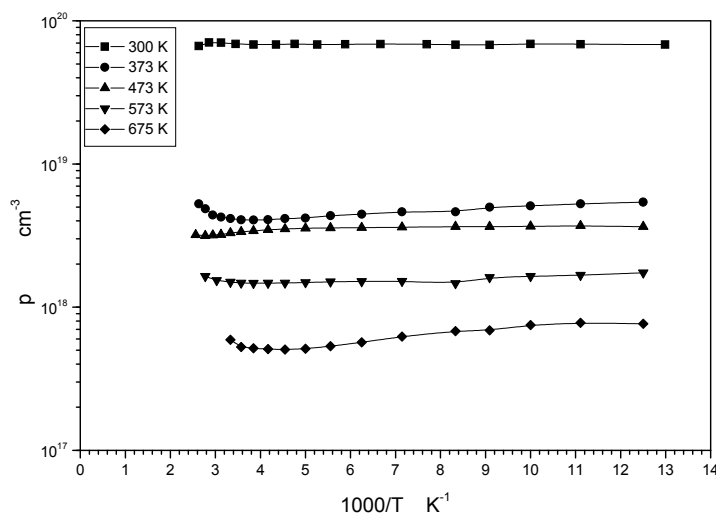


Fig. 5. Carriers concentration dependence upon substrate temperature for $Pb_{0.80}Sn_{0.20}Te$ films.

Positive Hall coefficient was observed in carriers concentration measurements for all films which indicate that p-type carriers are major. This agrees well with the observation of excess Te obtained from the EDX measurements. The carriers concentration decreases as the substrate temperature increases as shown in Fig.(5). It is observed that the charge carriers concentration slightly changes with cooling and it ranges between $8 \times 10^{19} \text{ cm}^{-3}$ and $5 \times 10^{17} \text{ cm}^{-3}$ as the substrate temperature increases, *i.e.* degeneracy of holes occurs especially at $T_s=300\text{-}473 \text{ K}$. The substrate temperature is considered as an effective parameter on the carrier's concentration. This decrease in carriers concentration is not only due to Te content but also from the defect density in the films. The carriers concentration decreases with substrate temperature increase may be due to the recrystallization process, which leads to the decrease of defects in the films during the film growth.

3.3 Optical Properties

A representative curve of the optical transmittance of the films deposited at substrate temperatures 673 K is shown in Fig.(6). The transmission curves are characterized by interference fringes. The optical transmission for the unheated substrate is small and includes high absorption especially in the long wavelength region. As the T_s increases, the optical transmission increases to $\sim 90 \%$. Free carriers absorption in the longer wavelength was checked for the absorption curves and found that the absorption coefficient is proportional to the square of the wavelength. The free carriers absorption process decreases sharply as the substrate temperature increases. This phenomenon agrees well with the decrement of the carriers concentration which affect on the free carriers absorption and consequently increases the transmittance curves as the substrate temperature increases. The calculated absorption coefficient, α , was used in the plot $(\alpha h\nu)^2$ vs $h\nu$ in order to determine the band gap from the intercept of the absorption edge as shown in Fig.(7). A red shift in the band gap shift was observed to be decreased as increasing the substrate temperature. Two mechanisms may affect on the band gap shift. They are the quantum confinement effect in nano crystalline materials and Burstein-Moss effect. As observed from the crystallite size dependence upon substrate temperature, the size in the range 50-80 nm is too long to make a change in the band gap. Normally at 15 nm, the energy gap confinement effect is vanished for most chalcogenides [15]. In the Burstein-Moss {BM} effect, the shift of the band gap is mainly due to high carriers concentration and/or lower effective mass. The shift was checked

using {BM} and found to be that the carriers concentration is responsible for band gap increasing. In this case, the minimum band gap is estimated using this model from $E_g-P^{2/3}$ relationship as shown in Fig.(8). P is the holes concentration. It was observed that the minimum E_g was found to be 0.194 eV. The calculated E_g from Eqn.(1) at composition 0.20 was 0.197 eV, which agrees well with the experimentally measured values. The value of E_g is near to the previously published values, which confirms the accuracy of this method of calculation.

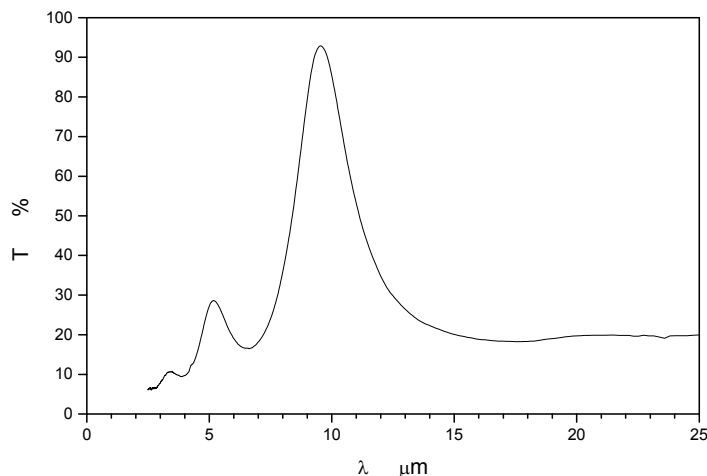


Fig. .6 Optical Transmission for $Pb_{0.8}Sn_{0.2}Te$ film deposited at $T_s = 673$ K.

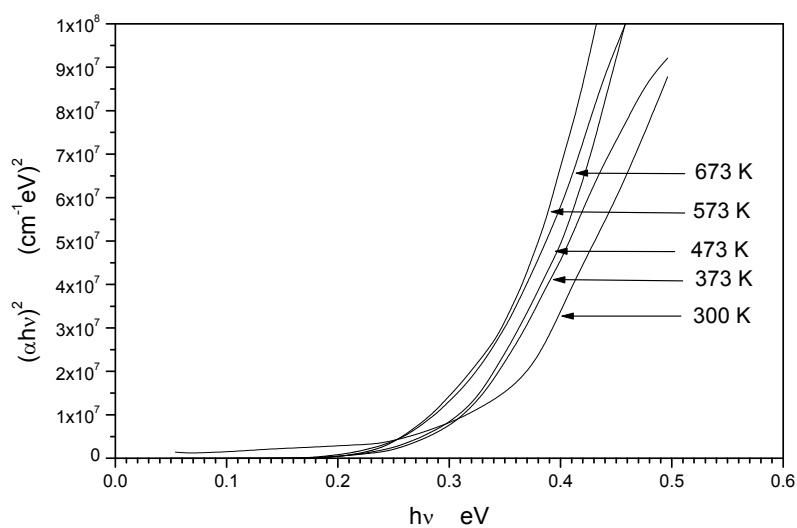


Fig. 7. $(\alpha hv)^2$ vs. $h\nu$ at different substrate temperature.

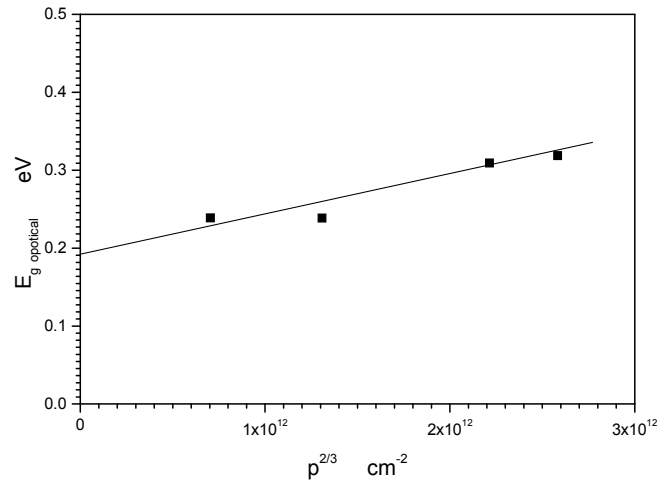


Fig. 8. Optical band gap dependence on the carrier concentration.

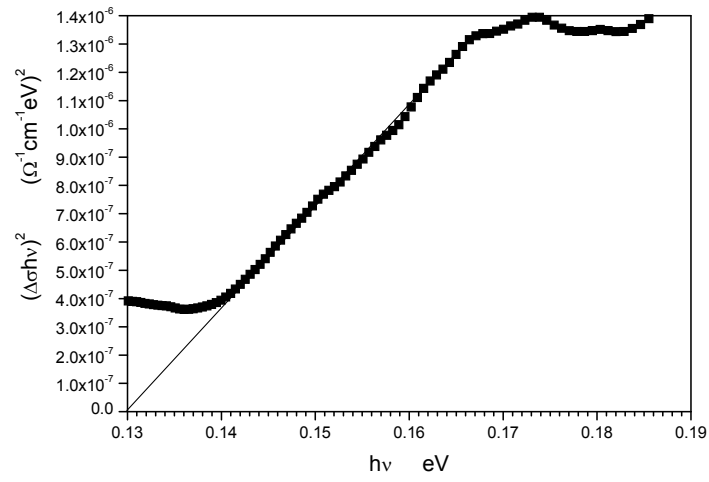


Fig. 9. $(\Delta\sigma hv)^2$ vs $h\nu$ 100 K and deposited at $T_s = 573$ K.

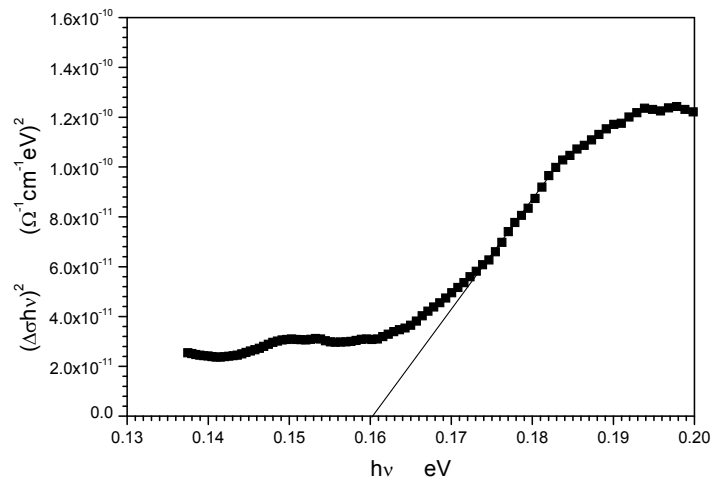


Fig. 10. $(\Delta\sigma hv)^2$ vs $h\nu$ 250 K and deposited at $T_s = 573$ K.

3.4 Photoconductivity

It is interesting to obtain the energy gap of $\text{Pb}_{0.8}\text{Sn}_{0.2}\text{Te}$ films from the photoconductivity, $\Delta\sigma$, measurements under monochromatic IR radiation at temperatures 100, 150, 200, 250 and 300 K. As representative curves Fig.(9) and Fig.(10) show the dependence of $(\Delta\sigma h\nu)^2$ vs $h\nu$ for deposited films at $T_s=573$ K and measured at 100 and 250 K. In the fundamental absorption region, the photoconductivity depends linearly upon the absorption coefficient. So that we use the plot $(\Delta\sigma h\nu)^2$ instead of $(\alpha h\nu)^2$. Table (3) shows the values of the E_g for films deposited at different T_s determined from the photoconductivity spectra. The deposited films at temperature 300 and 373 possess weak dependence upon temperature due to large Burstein-Moss effect. The deposited films at $T_s > 373$ possess the nearest values to $E(x,T)$ that are calculated from Eqn.(1) which are shown in Table(3). $T_s=573$ and 673 K show the best results.

4. Conclusions

The composition and Te content of the prepared $\text{Pb}_{0.8}\text{Sn}_{0.2}\text{Te}$ films at T_s in 300-673 K are close to the ingot materials which indicates that electron beam evaporation with substrate heating produces films with high quality and composition controlled. As the substrate temperature increases from 300-673 K, the electrical resistivity increases one order of magnitude in the high T_s range, the hole concentration increases 2-3 orders of magnitude and the Hall mobility increases by one order of magnitude. The optical transmittance increases $\approx 30\%$ to $\approx 100\%$. The energy gap was observed to be higher than the theoretical one due to Burstein-Moss shift for films prepared at lower substrate temperature which decreases as the substrate temperature increases. The energy gap obtained from the photoconductivity decreases also as T_s increases. At low measurement temperatures the theoretical and experimental E_g are close to each other due to the minimization of the carriers concentration and consequently decreasing the Burstein-Moss shift.

References

- [1] A. L. Dawar, P. Kumar, S. K. Paradkar, O. P. Tanjeja, P. C. Mathur, *Infrared Phys.* **32**, 133 (1982).
- [2] Marvin L. Cohen and Y. W. Tsang, "The Physics of Semimetals and Narrow Gap Semiconductors" proceeding of the Conference Held at Dallas, Texas in (20-21 March) **32**(1), 303 (1970).
- [3] T. F. Tao, C. C. Wang, *J. Nonmetals* **2**(1), 15 (1973).
- [4] S. P. Yordanov, Part I, *Bulgarian J. of Physics.*, **17**(6), 507 (1990).
- [5] S. P. Yordanov, Part II, *Bulgarian J. of Physics*, **18**(1), 15 (1991).
- [6] E. P. Skipetrov, A. N. Nekrasova, L. A. Skipetrova, L. I. Ryabova, *Proceeding of SPIE-"The International Society for Optical engineering"*, **3182**, 228 (1996).
- [7] U. V. Andreev, K. E. Geiman, E. A. Drabkin, A. V. Matveenko, Ye. A. Majaev and B. Ia. Moijee, *J. Physics and Technics of Semiconductors*, **9**(10), 1873 (1975) PP.
- [8] Kucherenko E. V, Kashirkaya L. M., *phys. Technics Semicond.* **9**(2), 209 (1975).
- [9] Ostrobordova V. V. and Terra F. S. *Bull Moscow Uni.* **30** (5)(1989).
- [10] Jay N. Zemel, James D. Jensen and R. B. Schooler, *Phys. Rev.* **140**(1A), A330 (1965).
- [11] *Springer Series in Optical Sciences: Optical and infrared Radiation*, R. H. Kingston, Springer-Verlag Berlin Heidelberg New York, (1978).
- [12] A. Maitre, R. Le. Toullec and M. Balkanski, *II international Conference on Physics of Semiconductors Proceeding.*, **2**, 826 (1972).
- [13] F.S. Terra, M. Abdel Rafea, M. Monir *Renewable Energy* **24**, 569 (2001).
- [14] F. S. Terra, M. Abdel Rafea, M. Monir *J. materials science. Mat. Elect.* **12**, 561 (2001).
- [15] M. Abdel Rafea, *J. materials science. . Mat. Elect.* **18**, 415 (2007).